SEMARAK ILMU PUBLISHING

Journal of Advanced Research in Fluid Mechanics and Thermal Sciences

Journal homepage:
https://semarakilmu.com.my/journals/index.php/fluid_mechanics_thermal_sciences/index
ISSN: 2289-7879

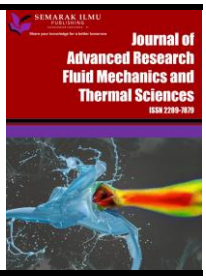

Performance Analysis of Solar Assisted Heat Pump Drying System with Dual Condensers

Ghaith Abusaibaa[1], Kamaruzzaman Sopian[1,*], Rohaimi Abdullah[1], Hasila Jarimi[1], Adnan Ibrahim[1]

[1] Solar Energy Research Institute, Universiti Kebangsaan Malaysia, 43600, Selangor, Malaysia

ARTICLE INFO

Article history:
Received 2 April 2022
Received in revised form 25 July 2022
Accepted 7 August 2022
Available online 3 September 2022

Keywords:
Heat pump; dryer; dual condensers; evacuated tubes; TRNSYS; EES simulation

ABSTRACT

The main components of the dual condenser solar-assisted heat pump (SAHP)drying include the solar collector, evaporator, compressor, fan coil, twin condensers, expansion valve, and drying chamber. The solar drying process was assisted by a heat pump, and the optimal efficiency was determined by heating and dehumidifying the air, and recirculating the air that has been heated. The efficiency of the heat pump system was assessed by its coefficient of performance (COP), which is the percentage of the actual heat delivered by the heat pump to the total electrical power necessary to operate the heat pump. The average temperature of the drying chamber reached a temperature of 60 °C with a relative humidity of around 70%, and the system's COP was 5.546 with no contribution from solar energy or at no solar fraction (SF = 0). The same conditions in the drying chamber can be achieved at solar faction or SF = 0.83, with COP increased to 12.7.

1. Introduction

Conventional and solar heat pump systems (SAHPS) have attracted the interest of energy experts because of their proven energy savings and their impact on the environment [1,2]. Green energy sources such as solar energy are used to assist the operation of heat pump drying systems for the preservation of food items derived from marine and agricultural resources [3]. This type of drying system has received great appreciation for its ability to create high-quality dried foods while simultaneously minimizing energy [4,5].

In an investigation by Hu *et al.,* on a SAHPD for wolfberry berries, they found that the heat pump's consumption of electrical energy decreased after adding solar assistance [6]. Dong *et al.,* investigated several coffee bean drying processes and found that the heat pump dryer preserved more ketones, phenols, and esters [7]. Also, Liu *et al.,* found that the adoption of heat pumps in the drying of mushrooms gave high-quality results, as the dried mushrooms had good color, a good smell, slight shrinkage in size, and the ability to mass-produce [8].

* *Corresponding author.*
E-mail address: ksopian@ukm.edu.my

https://doi.org/10.37934/arfmts.99.1.134148

The output of a solar photovoltaic thermal heat pump (SPV-THP) dryer for saffron processing under Qaen's meteorological conditions in Iran was investigated by Morttezapour *et al.,* [9]. A reduction in energy consumption of around 33% has been reported when using the PV air collector. The drying efficiency was calculated at 72%, and the maximum specific moisture extraction rate (SMER) was 1.16 kg/kWh at an airflow rate of 0.016 kg/s and at a drying temperature of 60 °C.

The efficiency of SPV-THP for drying applications was investigated by Şevik [10]. In this work, a hybrid photovoltaic thermal collector (PV-T) is used to assist the heat pump in heating the air. The heat pump working fluid is the R134a refrigerant, which is an environmentally friendly refrigerant. The temperature was controlled by means of the PID control system. The coefficient of performance (COP) values were estimated for the drying of various vegetables (mint, parsley, tomatoes) and fruits (strawberries). The estimated COP for mint was 2.28, parsley 2.17, tomatoes 1.96, and strawberries 2.27. The average thermal efficiency of the system was calculated and found to be within the range of 0.16 to 0.79, and the SMER value was in the same operating conditions within the range of 0.03 kg/kWh to 0.46 kg/kWh. Also, the energy use ratio for the same operating conditions was estimated in the range of 0.19 to 0.48.

The performance of a solar-assisted drier was also conducted by Ceylan and Güre [11]. The dryer's performance was evaluated for the drying of mint leaves. The air temperature of the heat pump condenser was reported to be 50 °C, while the air temperature from the solar collector was 45 °C. The system exergy efficiency was 0.26 and the system energy efficiency was 0.50, with the heat pump's ability to give a COP equal to 5.

The effectiveness of SAHPS for industrial heating purposes was investigated by Suleman *et al.,* [12]. The system comprises a heat pump cycle for the process of heating water and solar energy for another industrial heating process. The COP of the heat pump cycle was 3.54 and the exergy efficiency was 42.5%.

The SAHPS for the drying of mushrooms was conducted by Şevik *et al.,* [13]. The COP ranges from 2.1 to 3.1, with SMER ranging from 0.26 kg/kWh to 0.92 kg/kWh. The moisture content of the mushrooms was dried at a temperature of 45 ° C within the drying chamber, from an initial moisture content of 13.24 g water dry matter (dry basis) to a final moisture content of 0.07 g water dry matter (dry basis).

Qiu *et al.,* Examined the performance examination of SAHPS for drying 10 kg of radish in China [14]. In this system, the heating and cooling coils (main parts of the heat pump products) are combined with the drying chamber. In the SAHPS system, the COP were from 3.21 to 3.49 and reduced the amount of energy by 40.5% in relation to the heat and energy yield that was stored. The payback period for drying mushrooms, peppers, and radish in the life span of the system was determined to be 2 years, 4 years, and 6 years, respectively.

Li *et al.,* conducted theoretical and experimental studies on a SAHPS [15]. The results indicated that the solar fraction was 20% in normal climates and 28% during sunny days. The COP for the system and the average value for COP were 5.19 and 6.25, respectively, with a SMER of 3.0 kg/kWh. Further studies have indicated that SAHPS systems produce significantly higher product quality with a reduction in the amount of energy consumed by the heat pump compared with other existing systems [16].

The performance of a solar-ambient hybrid source heat pump drier (SAHSHPD) for copra drying under hot-humid weather conditions was conducted under meteorological conditions in Bulashi, India [17]. The results showed that the COP of a SAHSHPD varied between 2.31 and 2.77, with an average value of 2.54. The SMER was calculated as 0.79 kg/kWh. The moisture content (on a wet basis) of the copra was reduced from about 52% to about 9.2% and 9.8% in 40 h for trays at the

bottom and top, respectively. The COP was higher compared to a heat pump of ambient source for drying coconut pulp [18].

Hatem and Yumrutaş [19] created a computer model of a solar-powered heat pump and thermal energy storage (TES) tank used to dry wheat. MATLAB code was developed to simulate the performance metrics over time. After 10 years of operation with a wheat mass flow rate of 50 kg/h and a Carnot efficiency of 40%, the collector area, tank volume, COP, and SMER were 70 m^2 and 200 m^3, 4.43, 4.3, and 6.05, respectively.

Gu *et al.,* [20] developed a novel SAHPS for in-bin grain drying to address grain uniformity and drying time issues. The solar collector's thermal efficiency and the heat pump's COP were found to be 63 percent and 5.03 percent, respectively. After 42 hours of drying, 3,760 tonnes of grain had a water content of 12.5%. As a consequence, SAHPS grain drying costs fell from $5.57/t to $1.43/t.

Research investigations SAHPS dryers are limited and more empirical research and simulations are required to improve system efficiency. This study presents a new design of a smart heat pump dryer with a dual condenser and assisted with a solar evacuated tube collector system; it increases the COP of the SAHPS with a higher solar fraction.

2. Theoretical Model

2.1 Schematic (System Description)

The Solar Heat Pump Dryer (SHPD) using a double condenser and assisted with an evacuated tube collector (ETC) system was developed. The TRNSYS and EES programs were used to model and simulate the SHPD system, as illustrated in Figure 1 and 2. Figure 1 shows the SHPD device that was taken into consideration for this study. The ETC with storage tank system is connected to the heat pump through a heat exchanger.

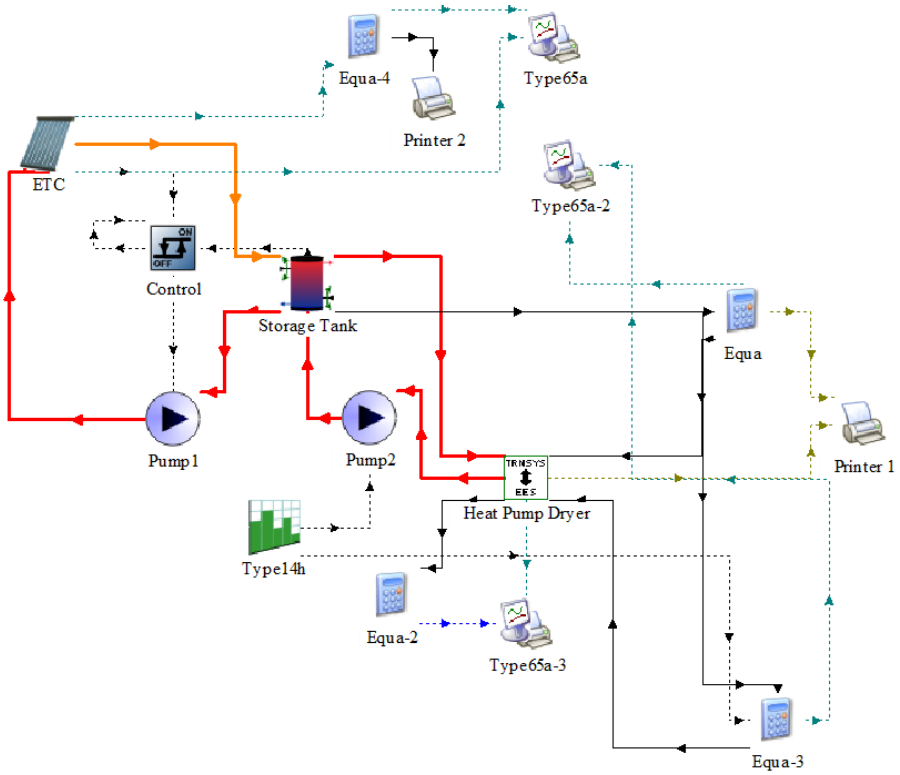

Fig. 1. TRNSYS model for heat pump dryer with a dual condenser and assisted with solar evacuated tube collector system

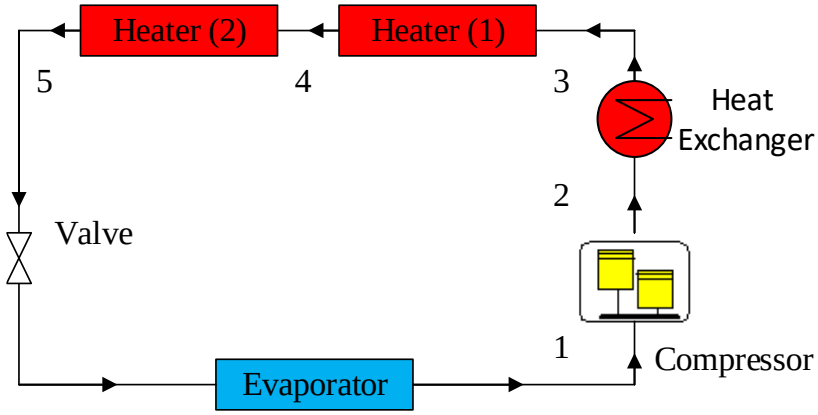

Fig. 2. EES Thermodynamic system

The ETC with the storage tank is connected to the heat pump in SHPD by the heat exchanger. The heat pump device is composed of the following components: the evaporator coil, pressure relief valve, freon compressor, and a double condenser with two fans per coil. He is transferred between water and R-32 refrigerant through the use of a heat exchanger. The heat pump receives energy from the solar collector. In the first and second condensing coils, an R-32 refrigerant absorbs additional heat from the solar collector and subsequently rejects this heat back into the atmosphere. The dryer's condenser coil fan expels this heat, which warms the dryer's interior to the required temperature. The R-32 refrigerant then travels via the expansion valve to the evaporator, where it completes the cycle. The operating period of the SHPD system in the simulation is from 8:00 to 18:00 in Kuala Lumpur, as shown in Figure 3.

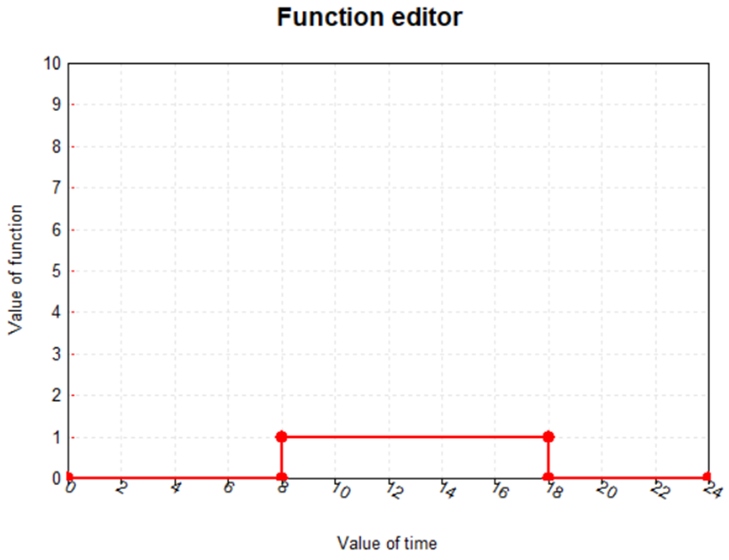

Fig. 3. Solar system operation period

2.2 The Thermodynamic Analysis

The useful energy gain Qu and the efficiency η of the ETC portion of the solar system are calculated as follows [21,22]

$$\eta = a_0 - a_1 \frac{(\Delta T)}{I_T} - a_2 \frac{(\Delta T)^2}{I_T} \quad (1)$$

$$Q_u = m_{dot} * C_p * (T_{out} - T_{in}) \quad (2)$$

A_o is the intercept (maximum) of the collector efficiency, a_1 is the negative of the first-order coefficient in collector efficiency equation, a_2 is the negative of the second order coefficient in collector efficiency equation. I_T is the global radiation incident on the solar collector on a tilted surface.

The Coefficient of Performance (COP) and Solar fraction (SF) are defined as follows

$$COP_{HP} = Q_{con}/W_{comp} \quad (3)$$

$$Q_{con} = m_{dot} * C_p * \Delta T \quad (4)$$

$$SF = Q_u/W_{comp} \quad (5)$$

3. Parametric Analysis

3.1 Solar System

The important parameters for the design of the parts of the solar system were modeled by the TRNSYS program, which are the ETC slope, the volume of the storage tank, and the velocity of water flow in the solar system.

The efficacy of the ETC tilt angle towards south has been investigated. In principle, the ETC region's latitude should be the ideal value of the ETC slope for ETC without a tracking mechanism. In Figure 4, the ETC slope was altered from 0° to 90°. The results showed that the optimum possible collection energy acquires an angle of slope equal to the latitude in the area. As a result, the collector's ideal slope in Kuala Lumpur, Malaysia, at 3.14°N latitude, is 0°N.

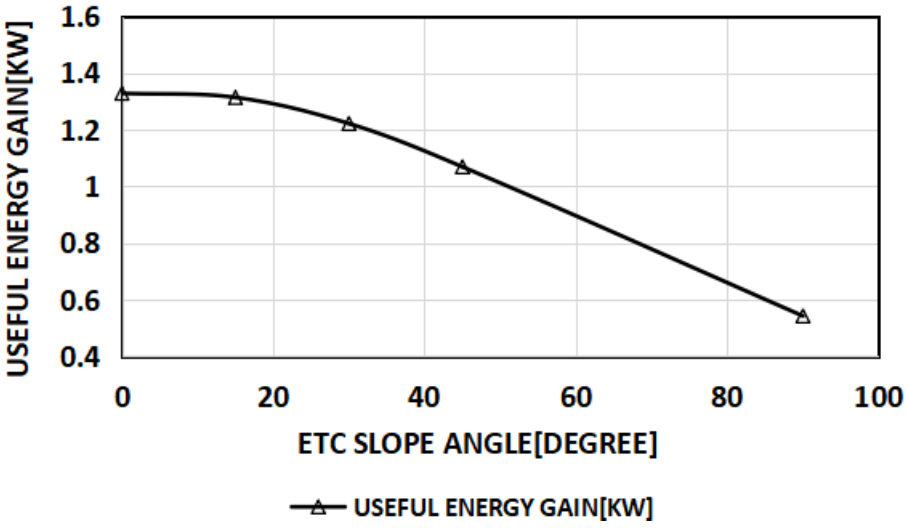

Fig. 4. ETC slope vs. UEG

3.2 Storage Tank Volume Flow Rate

The optimum hot water storage tank (HWST) is selected by considering how volume flow rate (VFR) storage affects system performance. For this purpose, HWST with VFR varies from 0.1 m^3/s to 0.5 m^3/s. Based on the analysis of HWST parameters with VFR, the maximum attained between the

trend solar fraction and the trend of annual energy rate to load would be the optimal VFR of HWST (ERL). By observing the trend, this result was demonstrated in Figure 3. The thermal energy delivered to the dryer system generator load from UEG is computed using the solar fraction (SF). Figure 5 depicts data from Kuala Lumpur, Malaysia. SF = (UEG)/(Generator load). The HWST, with a VFR of 0.325 m^3/s, achieved the minimum trend of annual heat pump power with the highest SF and ERL.

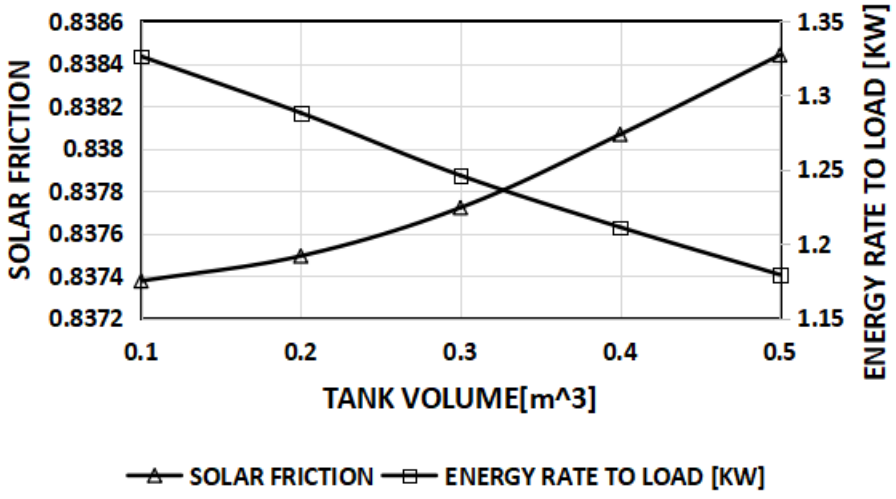

Fig. 5. SF and Annual useful solar power vs. VFR of HWST

3.3 Mass Flow Rate

The effectiveness of changing the mass flow rate (MFR) of ETC is investigated, with the MFR of ETC being changed from 30 to 300 kg/hr. It is shown in Figure 6. The ETC MFR of 180 kg/h improves the SF of Kuala Lumpur, Malaysia by up to 0.74 %. In this optimization, it was considered the ultimate suitable amount. While it is remarkable to indicate that a change in the MFR with a range of 30 to 300 kg/h was not a big change in the annual SF, it's been in diversity with a range of 0.69 % to 0.74 % for Kuala Lumpur, Malaysia. The ultimate system requirements for the Kuala Lumpur, Malaysia optimizing study consisted of a 6 m2 ETC area and a number of ETC tilted at 0^o for Kuala Lumpur, Malaysia from the horizontal and with 180 kg/h MFR and a 0.325 m3 HWST. The efficient dryer requires 1.6 hp.

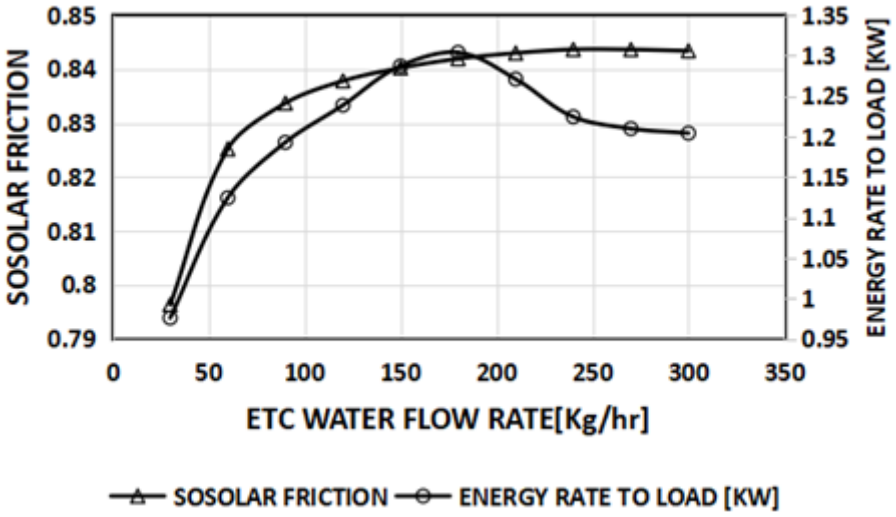

Fig. 6. SF and ERL vs. MFR of ETC

The parameters for the components of the solar system, a south-facing ETC with a tilted angle of 0° with an area of 6 m^2. ETC and SHPD's maximum flow rates are set at 180 kg/h and 200 kg/h, respectively. The volume of the storage tank is estimated as 0.325 m3.

3.4 Dryer Structure

The main model of the dryer structure was designed and built by the Solid Work program. Figure 7 shows the external dimensions and the distribution of the internal parts of the heat pump, represented by the first condenser, the second condenser, and the evaporator.

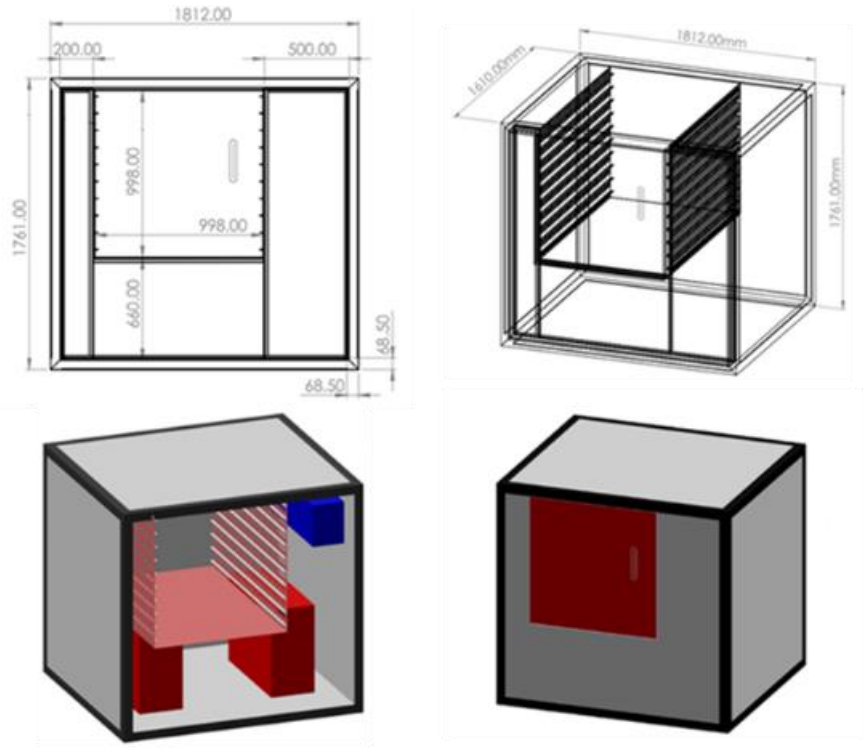

Fig. 7. dryer structure

3.5 Air Cycle Design

The holes and the speed of dry air passing through these holes were designed to withdraw moisture from being dried in a closed cycle by the COMSOL program. This part of the design has been taken care of because air velocity has a significant impact on the drying quality [23]. The test case is holes of equal diameters, and the diameter of each of these holes is 0.03 meters. Figure 8 shows the air velocity distribution over the holes and the flow of air during the cycle. Moreover, the curve in Figure 9 shows the gradient of the velocity of dry air when changing the number of holes within a range from 1 to 10, where the last gradient gave the best flowability for air velocity, where the results show that the best flow for dry air velocity was when the number of holes was 10 and the speed of dry air was 2.85 m/sec.

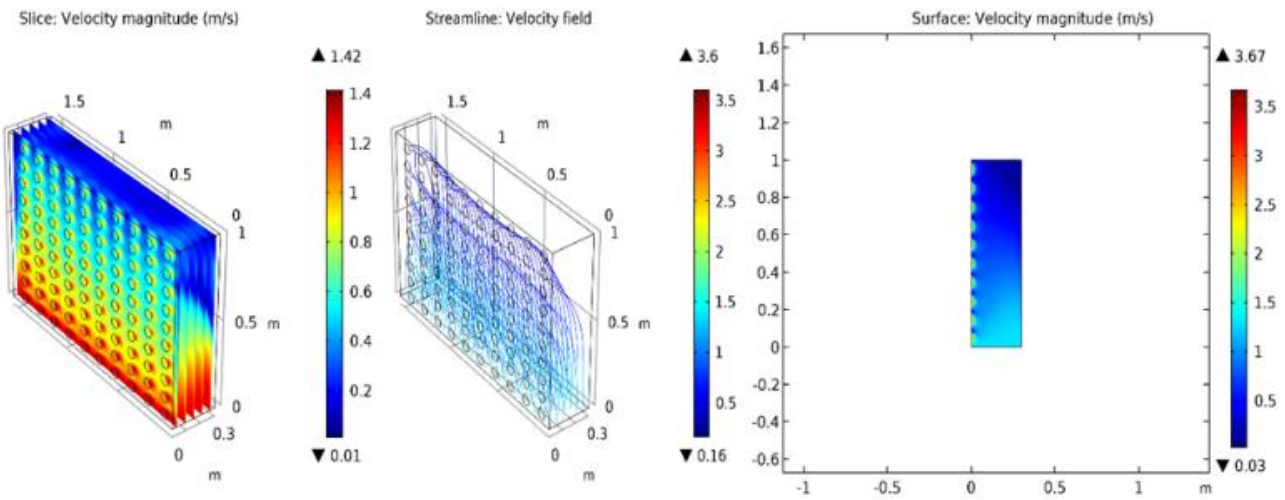

Fig. 8. The air velocity distribution over the holes

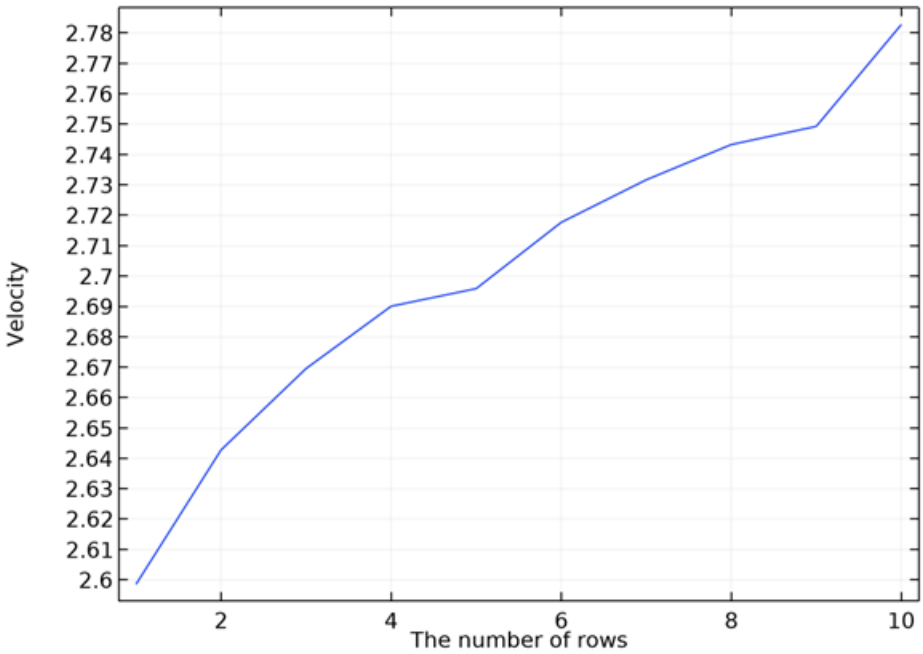

Fig. 9. The gradient of the velocity of dry air when changing the number of holes

3.6 Dryer System

The modeling of the Smart-Heat Pump Dryer system was conducted with the EES program. Figure 10 illustrates the EES model for a Smart-Heat Pump Dryer with a dual condenser with the drying process in terms of temperature and humidity in the dryer chamber at night or in the absence of solar radiation when the SF is zero, while figure 11 illustrates the EES model for the same system at midday when the SF reaches its maximum value of 83%.

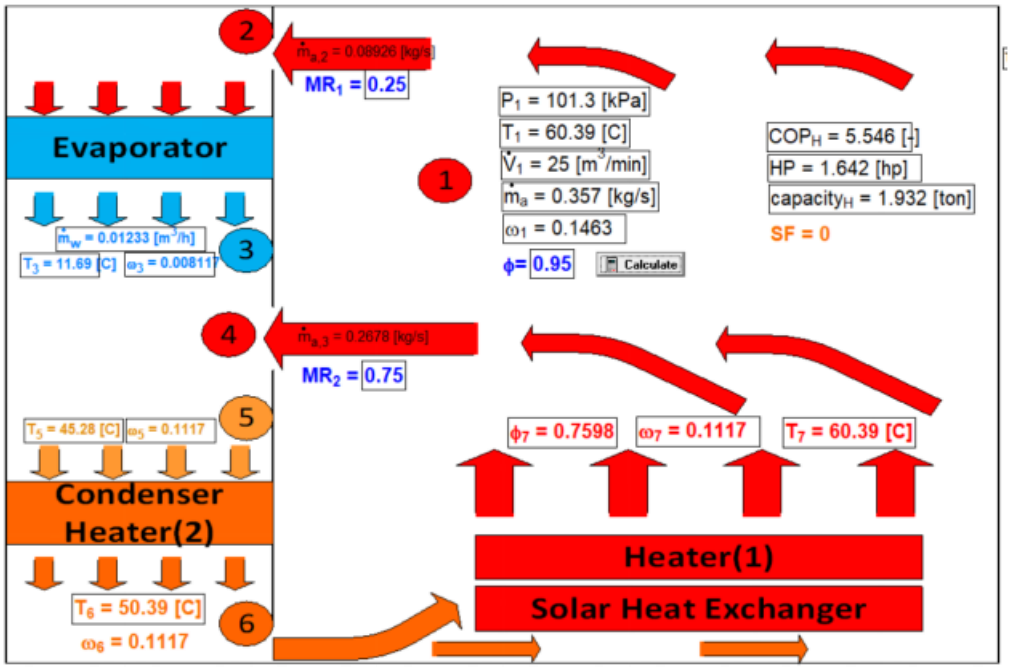

Fig. 10. EES model without solar energy

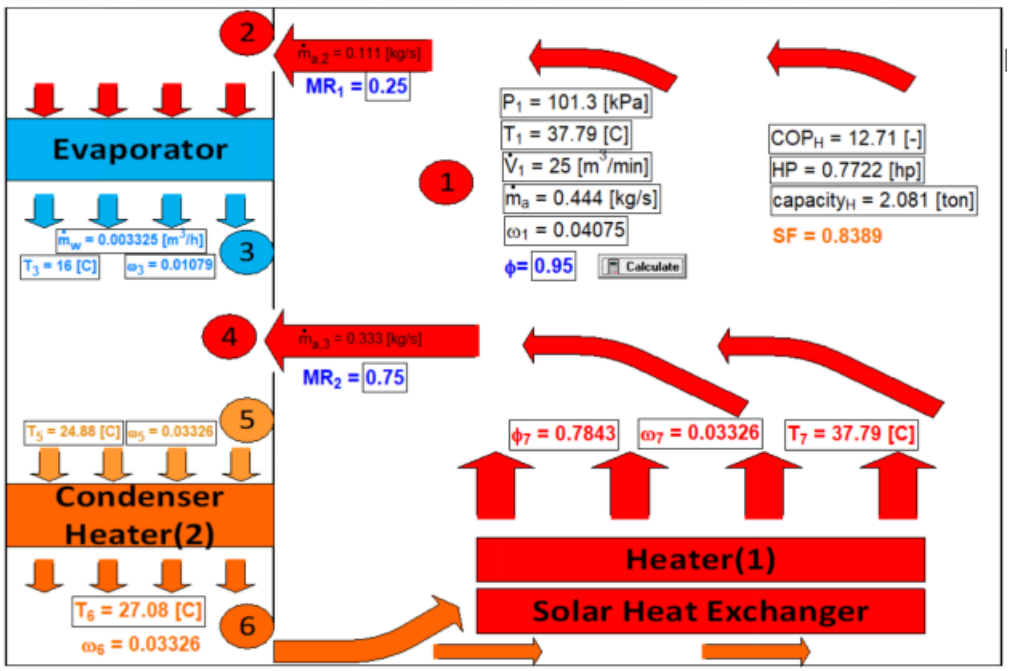

Fig. 11. EES model with solar energy

4. Results and Observations

The SHPD and ETC were combined, and the ETC was the primary source of hot water for the dryer via a heat exchanger. Moreover, it decreases the heat pump's electricity usage. The heat pump in the dryer will be triggered when there is minimal solar radiation or at night.

Three days of the simulation were used on January 13th, 14th, and 15th, with a one-hour time step Figure 12 illustrates the maximum energy value provided by the storage tank from ETC to the SHPD, which is roughly 3.215 kW at 2.00 PM.

The first parameter to be considered was the ETC outlet hot water temperature. During the starting process, it takes a while to warm up the system. Hence, the curve is flat as can be seen from the bottom left side of Figure 13. At around 8:00 AM, when the intensity of radiation is high, around 59.59 °C was obtained. At a certain point in the high solar time, for instance, at 13:00, a maximum temperature of 93.25 °C obtained. Furthermore, the system has effectively accumulated energy for the period of ten hours from 8.00 AM to 6.00 PM.

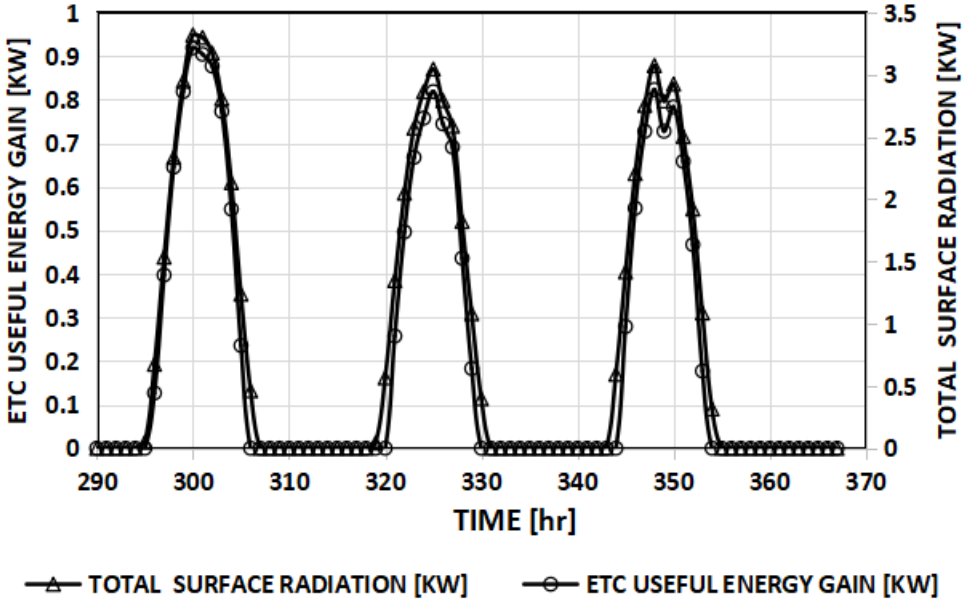

Fig. 12. Useful energy gain simulation

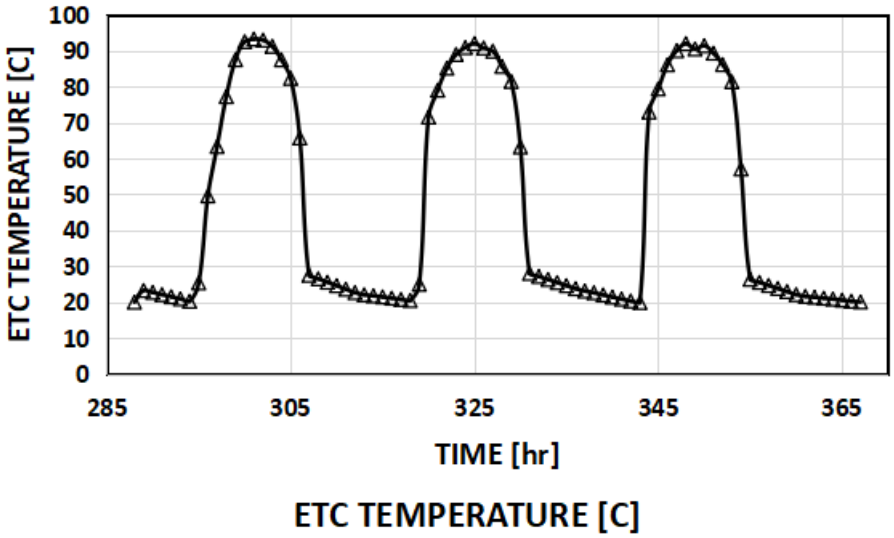

Fig. 13. Temperature outlet of ETC plot for Kuala Lumpur, Malaysia

Figure 14 shows that the energy delivered by the heater is the highest possible at the beginning of operation of the system between 10.00 AM and 1.00 PM as well as at the end of the working of SEAC between 4.00 PM to 6.00 PM. It has been noted that HWST maintains the non-fluctuation energy of the solar collector, which goes through HWST to the dryer system. Hence, HWST can supply stable to the dryer which has a volume of 0.325 m^3

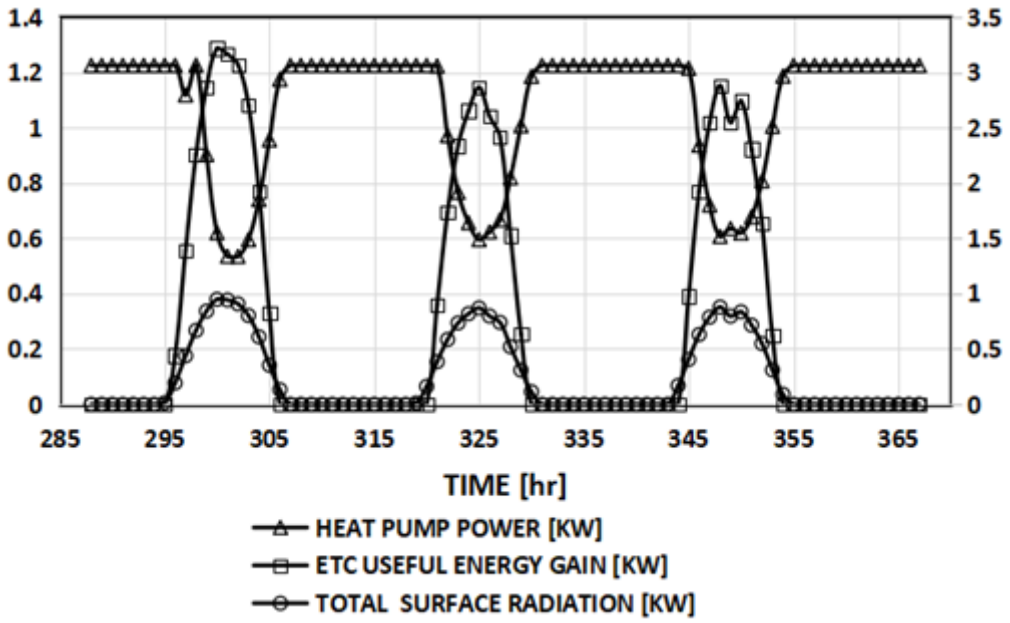

Fig. 14. Outlet energy for Kuala Lumpur, Malaysia

Figure 14 shows that the lowest and highest values of the heat pump power range between 0.534 kW and 1.226 kW, respectively. Furthermore, the UEG energy provided by ETC for the drying system ranges between 0 and 3.215 kW, respectively. The values of solar irradiance in the same time period range between 0 and 0.948 kW/m^2 respectively.

Figure 15 shows the efficiency of ETC, which reaches 0.57 %, which allows it to meet the demand for hot water needed by the drying system. This leads to reduction of the electricity consumption, hence saving money and contributing to reducing CO_2 emissions resulting from the consumption of electricity using fossil fuels.

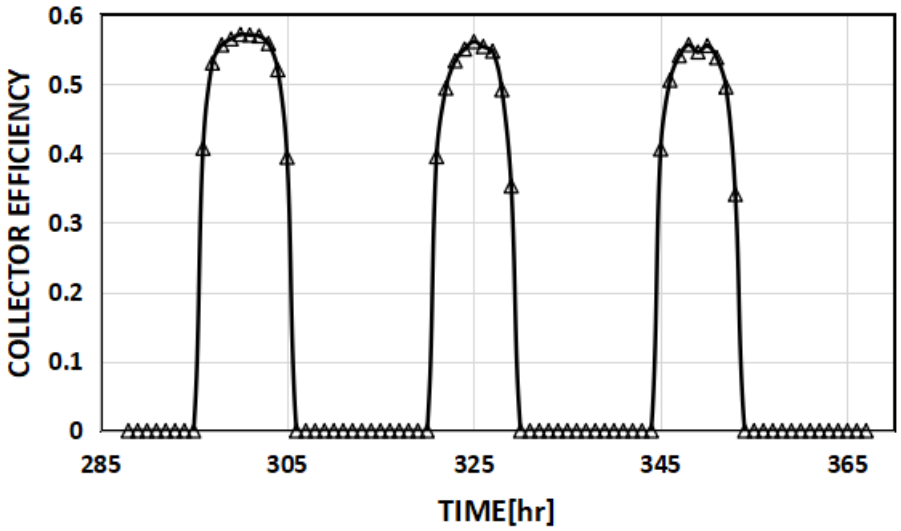

Fig. 15. ETC Efficiency

Figure 16 shows the peak value of SF is about 83 % at 2.00 PM. Figure 17 shows that the maximum and lowest values of COP_{hp} were roughly 12.7 at 2.00 PM and 5.54 PM at sunset. The P-h diagrams for the SHPD cycle in the absence of solar energy and in the presence of solar energy are shown in Figures 18 and 19, respectively.

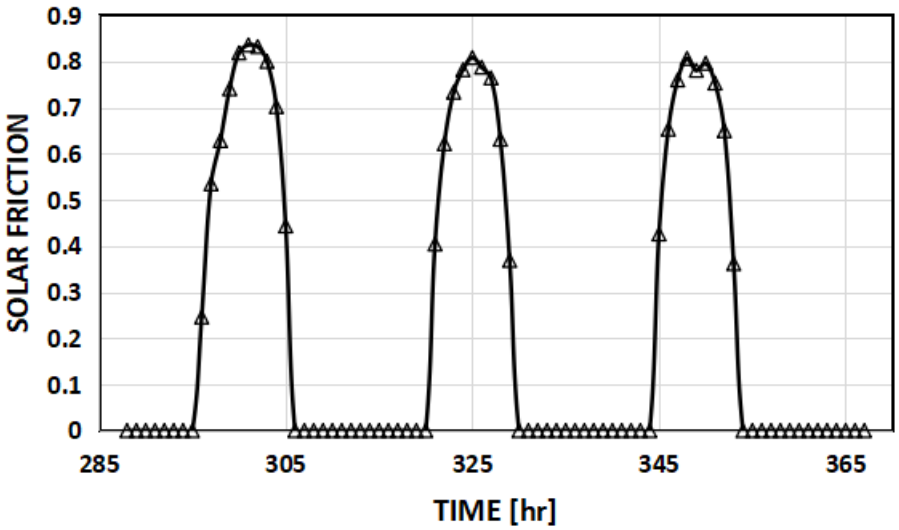

Fig. 16. Simulation SF with Time

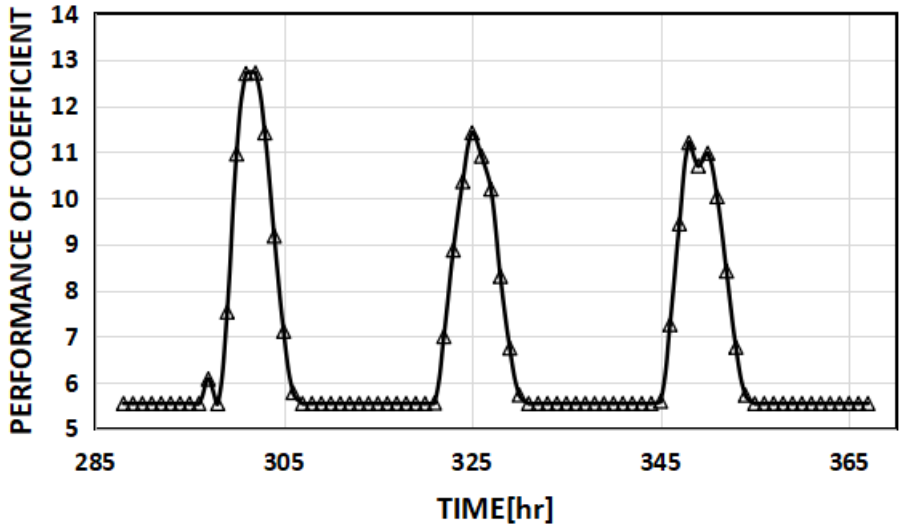

Fig. 17. Simulation COP_{hp}, with Time

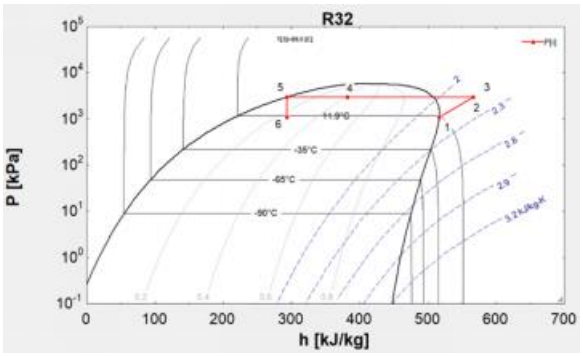

Fig. 18. P-h diagram without solar energy

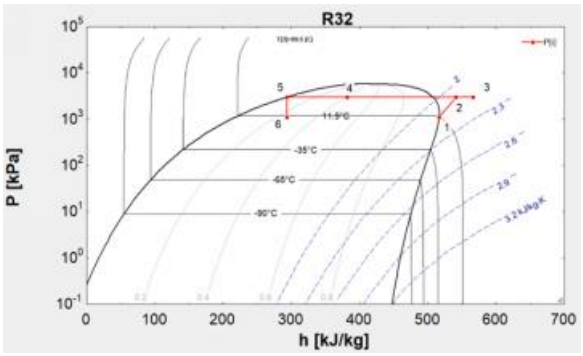

Fig. 19. P-h diagram with solar energy

The temperature of the dryer chamber is the following important parameter: The hot water is supplied to the dryer system and released as hot air. During the system's working hours of 8.00 AM to 6.00 PM., the dryer system remains operational. Because of the use of solar energy during this

time period and the savings in electricity consumed. Figure 20 shows that the temperature of the constantly drying chamber is between 55 °C and 60 °C.

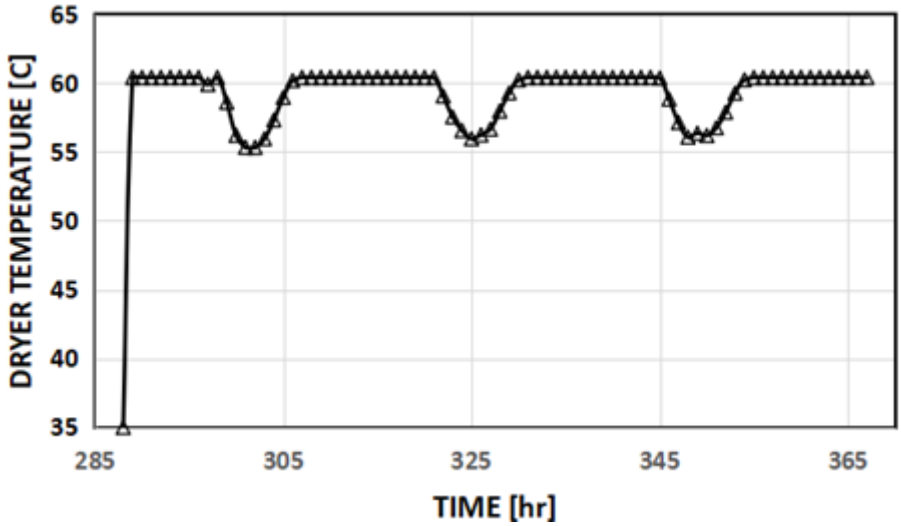

Fig. 20. Dryer chamber temperature

Mint leaves with an intial weight of 50 kg were tested. Figure 21 shows a simulation of the humidity curve during the five-hour test period, also known as the drying curves. As can be seen from the curve that the humidity was at the highest value 99% at the beginning of the operation, and then humidity decreased during the drying process of material Mint leaves, until it reached its lowest level, which was 15 %, which led to the withdrawal of 35 kg of moisture in material Mint leaves.

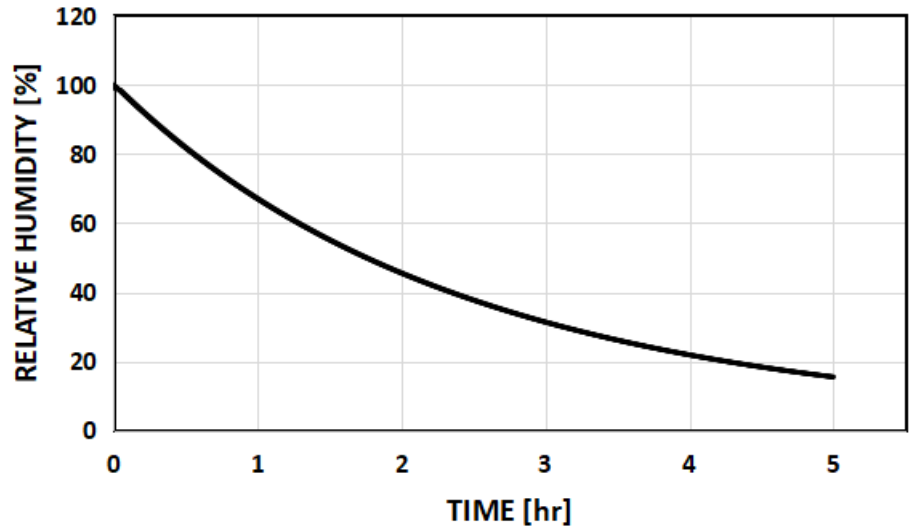

Fig. 21. Drying Curves of Mint leaves

5. Conclusions

The SHPD system was simulated using TRNSYS and the Kuala Lumpur climate conditions. An ETC size of 6 m^2 and slanted at a 0-degree angle from the horizontal were found to be the best solutions for HWST. ETC's storage tank provides the most energy to the SHPD around 2.00 PM., about 3.215 KW. At 2 p.m., SF reaches its peak value of almost 83%. At 2 PM, COP was at its peak value, which was around 12.7, while the COP system had its lowest value at sunset, which was 5.54. It was found

that adding a second condenser had a considerable positive impact on increasing the value of COP and, as a result, on increasing the overall efficiency of the dryer's operations. The decrease in power usage that this system has produced lessens reliance on energy sources that exacerbate global warming by emitting hazardous pollutants into the atmosphere. The findings of this study show that SHPD may be used in Malaysian climatic conditions, as well as provide an impetus for additional research within the SHPD framework.

Acknowledgement
The authors would like to thank the Universiti Kebangsaan Malaysia for the grant MRUN -RAKAN RU-2019-001/1 to support this work. Additionally, this work has been accepted and presented at the ICE-SEAM 2021.

References

[1] Nukulwar, Masnaji R., and Vinod B. Tungikar. "Recent Development of the Solar Dryer integrated with thermal energy storage and auxiliary units." *Thermal Science and Engineering Progress* (2022): 101192. https://doi.org/10.1016/j.tsep.2021.101192

[2] Hamid, Khalid, Uzair Sajjad, Kai Shing Yang, Shih-Kuo Wu, and Chi-Chuan Wang. "Assessment of an energy efficient closed loop heat pump dryer for high moisture contents materials: An experimental investigation and AI based modelling." *Energy* 238 (2022): 121819. https://doi.org/10.1016/j.energy.2021.121819

[3] Safri, Nurul Aiman Mhd, Zalita Zainuddin, Mohd Syahriman Mohd Azmi, Idris Zulkifle, Ahmad Fudholi, Mohd Hafidz Ruslan, and Kamaruzzaman Sopian. "Current status of solar-assisted greenhouse drying systems for drying industry (food materials and agricultural crops)." *Trends in Food Science & Technology* 114 (2021): 633-657. https://doi.org/10.1016/j.tifs.2021.05.035

[4] Colak, Neslihan, and Arif Hepbasli. "A review of heat pump drying: Part 1–Systems, models and studies." *Energy conversion and management* 50, no. 9 (2009): 2180-2186. https://doi.org/10.1016/j.enconman.2009.04.031

[5] Li, Jin, Ying Zhang, Ming Li, Yunfeng Wang, Mingyuan Shi, Meng Gao, Zhihan Deng, Gansong Lu, and Rui Liu. "Study on heating performance of solar-assisted heat pump drying system under large temperature difference." *Solar Energy* 229 (2021): 148-161. https://doi.org/10.1016/j.solener.2021.08.038

[6] Hu, Zhongting, Sheng Zhang, Wenfeng Chu, Wei He, Cairui Yu, and Hancheng Yu. "Numerical analysis and preliminary experiment of a solar assisted heat pump drying system for Chinese wolfberry." *Energies* 13, no. 17 (2020): 4306. https://doi.org/10.3390/en13174306

[7] Dong, Wenjiang, Rongsuo Hu, Yuzhou Long, Hehe Li, Yanjun Zhang, Kexue Zhu, and Zhong Chu. "Comparative evaluation of the volatile profiles and taste properties of roasted coffee beans as affected by drying method and detected by electronic nose, electronic tongue, and HS-SPME-GC-MS." *Food chemistry* 272 (2019): 723-731. https://doi.org/10.1016/j.foodchem.2018.08.068

[8] Liu, Yin, Kun-Zheng Zhao, Man Jiu, and Yan Zhang. "A heat pump system for Lentinula edodes drying and its drying property." *Thermal Science* 22, no. 4 (2018): 1759-1764. https://doi.org/10.2298/TSCI1804759L

[9] Mortezapour, Hamid, Barat Ghobadian, Saeid Minaei, and Mohammad Hadi Khoshtaghaza. "Saffron drying with a heat pump–assisted hybrid photovoltaic–thermal solar dryer." *Drying Technology* 30, no. 6 (2012): 560-566. https://doi.org/10.1080/07373937.2011.645261

[10] Şevik, Seyfi. "Experimental investigation of a new design solar-heat pump dryer under the different climatic conditions and drying behavior of selected products." *Solar Energy* 105 (2014): 190-205. https://doi.org/10.1016/j.solener.2014.03.037

[11] Ceylan, İlhan, and Ali Etem Gürel. "Solar-assisted fluidized bed dryer integrated with a heat pump for mint leaves." *Applied Thermal Engineering* 106 (2016): 899-905. https://doi.org/10.1016/j.applthermaleng.2016.06.077

[12] Suleman, F., I. Dincer, and M. Agelin-Chaab. "Energy and exergy analyses of an integrated solar heat pump system." *Applied Thermal Engineering* 73, no. 1 (2014): 559-566. https://doi.org/10.1016/j.applthermaleng.2014.08.006

[13] Şevik, Seyfi, Mustafa Aktaş, Hikmet Doğan, and Saim Koçak. "Mushroom drying with solar assisted heat pump system." *Energy Conversion and Management* 72 (2013): 171-178. https://doi.org/10.1016/j.enconman.2012.09.035

[14] Qiu, Yu, Ming Li, Reda Hassanien Emam Hassanien, Yunfeng Wang, Xi Luo, and Qiongfen Yu. "Performance and operation mode analysis of a heat recovery and thermal storage solar-assisted heat pump drying system." *Solar Energy* 137 (2016): 225-235. https://doi.org/10.1016/j.solener.2016.08.016

[15] Li, Y., H. F. Li, Y. J. Dai, S. F. Gao, Lei Wei, Z. L. Li, I. G. Odinez, and R. Z. Wang. "Experimental investigation on a solar assisted heat pump in-store drying system." *Applied Thermal Engineering* 31, no. 10 (2011): 1718-1724. https://doi.org/10.1016/j.applthermaleng.2011.02.014

[16] Li, Haifeng, Yanjun Dai, Jianguo Dai, Xibo Wang, and Lei Wei. "A solar assisted heat pump drying system for grain in-store drying." *Frontiers of Energy and Power Engineering in China* 4, no. 3 (2010): 386-391. https://doi.org/10.1007/s11708-010-0003-3

[17] Mohanraj, M. "Performance of a solar-ambient hybrid source heat pump drier for copra drying under hot-humid weather conditions." *Energy for Sustainable Development* 23 (2014): 165-169. https://doi.org/10.1016/j.esd.2014.09.001

[18] Mohanraj, M., P. Chandrasekar, and V. V. Sreenarayanan. "Performance of a heat pump drier for copra drying." *Proceedings of the Institution of Mechanical Engineers, Part A: Journal of Power and Energy* 222, no. 3 (2008): 283-287. https://doi.org/10.1243/09576509JPE548

[19] Ismaeel, Hatem Hasan, and Recep Yumrutaş. "Investigation of a solar assisted heat pump wheat drying system with underground thermal energy storage tank." *Solar Energy* 199 (2020): 538-551. https://doi.org/10.1016/j.solener.2020.02.022

[20] Gu, Xinzhuang, Jianguo Dai, Haifeng Li, and Yanjun Dai. "Experimental and theoretical assessment of a solar assisted heat pump system for in-bin grain drying: A comprehensive case study." *Renewable Energy* 181 (2022): 426-444. https://doi.org/10.1016/j.renene.2021.09.049

[21] McIntire, William R. "Factored approximations for biaxial incident angle modifiers." *Solar Energy* 29, no. 4 (1982): 315-322. https://doi.org/10.1016/0038-092X(82)90246-8

[22] Theunissen, P-H., and W. A. Beckman. "Solar transmittance characteristics of evacuated tubular collectors with diffuse back reflectors." *Solar energy* 35, no. 4 (1985): 311-320. https://doi.org/10.1016/0038-092X(85)90139-2

[23] Budiyanto, Muhammad Arif. "Effect of Variation Inlet Velocity to the Cooling Speed Capacity Inside a Refrigerated Container." *Journal of Advanced Research in Numerical Heat Transfer* 2, no. 1 (2020): 14-20.

[24] Steen, M. "Greenhouse gas emissions from fossil fuel fired power generation systems." *Institute for Advanced Materials, Joint Research Centre, European Commission* (2000).